Nuclear Materials and Energy 31 (2022) 101198

Contents lists available at ScienceDirect

Nuclear Materials and Energy

journal homepage: www.elsevier.com/locate/nme

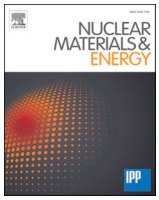

# Effect on impact properties of adding tantalum to V-4Cr-4Ti ternary vanadium alloy

Takeshi Miyazawa [a,d,*], Haruka Saito [a], Yoshimitsu Hishinuma [b], Takuya Nagasaka [b], Takeo Muroga [b], Jingjie Shen [b], Yasuki Okuno [c], Hao Yu [c], Ryuta Kasada [c], Akira Hasegawa [d]

[a] Tohoku University, Sendai 980-8579, Japan
[b] National Institute for Fusion Science, Toki, Gifu 509-5292, Japan
[c] Institute for Materials Research, Tohoku University, Sendai 980-8577, Japan
[d] Current Affiliation: Japan Atomic Energy Agency, Oarai, Ibaraki 311-1393, Japan

ARTICLE INFO

*Keywords:*
Blanket structural materials
Impact properties
Solid solution strengthening

ABSTRACT

Four V-Ta-4Cr-4Ti quaternary alloys containing different quantities of Ta were investigated to determine the effect of Ta content on the Charpy impact properties. Five button-shaped ingots of the V-4Cr-4Ti ternary alloy and V-*x*Ta-4Cr-4Ti quaternary alloys ($x$ = 3, 9, 15, and 22 wt.%) were fabricated on a laboratory scale by using non-consumable arc-melting in an argon atmosphere. Charpy impact tests were conducted at temperatures ranging from 77 K to 293 K using an instrumented impact tester. Both the upper shelf energy and the ductile–brittle transition temperature increased with increasing Ta content. The addition of 3 wt.% Ta resulted in solid solution strengthening without any degradation of the Charpy impact properties. Thus, the addition of 3 wt.% Ta (V-3Ta-4Cr-4Ti) is an appropriate amount to use in blanket structural materials for nuclear fusion reactors. The spectra of TEM-EDS for V-3Ta-4Cr-4Ti quaternary alloy indicate that there is no significant enrichment of Ta in the matrix as compared with that in the precipitate. However, thermal aging may result in the formation of the Laves phase, causing the degradation of Charpy impact properties. The characterization of precipitates, thermal aging, and creep tests of the V-3Ta-4Cr-4Ti quaternary alloy need to be investigated to determine the optimum Ta content.

## 1. Introduction

Vanadium(V)-based alloys are attractive structural materials for blanket systems in advanced fusion reactors owing to their potentially low-induced activation characteristics, superior high temperature strength, and excellent resistance against neutron irradiation damage [1–3]. A V-based alloy nominally containing 4 wt.% Cr and 4 wt.% Ti (V-4Cr-4Ti ternary alloy), which has favorable impact properties, has been selected as the leading candidate for this application [4–6]. The creep rupture strength is one of the key issues to determine the upper operating temperature, which is currently assumed to be approximately 973 K for V-4Cr-4Ti ternary alloy [7]. Although a higher Cr content can improve the creep rupture strength of V-Cr-Ti alloys through solid solution strengthening [8], it may also lead to an increase in the ductile-to-brittle transition temperature (DBTT) and degradation of fabricability [9,10]. The effects of tantalum (Ta) addition on the tensile properties and rolling fabricabilities of V-4Cr-4Ti ternary alloys have been previously investigated [11]. Ta has relatively low levels of long-lived radioactivity after neutron irradiation through fusion [12]. The Ta addition to V-4Cr-4Ti ternary alloy can improve their tensile strengths without degrading their rolling fabricabilities. Although the addition of Ta significantly improves tensile properties such as solid solution strengthening [11,13–16], the impact properties of V-Ta-4Cr-4Ti quaternary alloys have not yet been studied. The purpose of the present study is to study the effect of Ta addition on the impact properties of V-4Cr-4Ti ternary alloy for use as blanket structural materials in advanced fusion reactors.

## 2. Materials and experimental methods

Table 1 lists the chemical compositions of a V-4Cr-4Ti ternary alloy and four V-Ta-4Cr-4Ti quaternary alloys examined in this study. The quantity of interstitial impurities such as O, N, and C in the V-Ta-4Cr-4Ti quaternary alloys were controlled to give the same levels as those

* Corresponding author.
*E-mail address:* miyazawa.takeshi@jaea.go.jp (T. Miyazawa).

https://doi.org/10.1016/j.nme.2022.101198
Received 28 February 2022; Received in revised form 27 April 2022; Accepted 5 May 2022
Available online 10 May 2022

**Table 1**
Chemical compositions of the examined alloys (wt.%).

| Code | V | Ta | Cr | Ti | C | N | O |
|---|---|---|---|---|---|---|---|
| V-4Cr-4Ti | bal. | < 0.01 | 3.86 | 4.04 | 0.009 | 0.008 | 0.009 |
| V-3Ta-4Cr-4Ti | bal. | 3.23 | 3.88 | 4.03 | 0.010 | 0.009 | 0.009 |
| V-9Ta-4Cr-4Ti | bal. | 9.20 | 3.89 | 4.05 | 0.010 | 0.006 | 0.008 |
| V-15Ta-4Cr-4Ti | bal. | 14.6 | 3.84 | 3.99 | 0.009 | 0.004 | 0.008 |
| V-22Ta-4Cr-4Ti | bal. | 21.9 | 3.86 | 4.02 | 0.009 | 0.008 | 0.007 |

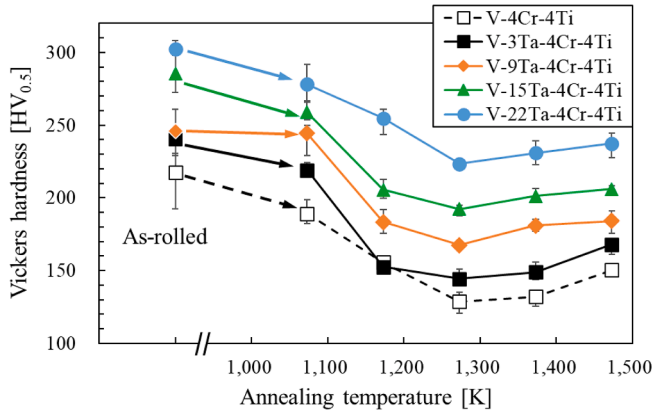


**Fig. 1.** Recovery of hardness as a function of the annealing temperature after cold rolling.

observed in the high-purity V-4Cr-4Ti reference alloy known as NIFS-HEAT-2 [17,18]. Five different alloys consisting of V-4Cr-4Ti and V-*x*Ta-4Cr-4Ti ($x$ = 3, 9, 15, and 22 wt.%) were fabricated using a non-consumable arc-melting method in an Ar atmosphere to obtain button-shaped ingots of approximately 30 g each. The V-22Ta-4Cr-4Ti alloy contained 7.3 at.% of Ta content, which was below the solid solubility limit of a Laves phase ($V_2Ta$) in the V-Ta phase diagram [19]. The button-shaped ingots were cold-rolled into sheets with a thickness of 2 mm, representing an approximately 80 % reduction in thickness.

The sheet specimens for Vickers microhardness measurements were cut from the alloy sheets, mechanically and electrolytically polished, and then annealed at 1073–1473 K for 1 h under a pressure of less than 1 $\times$ $10^{-3}$ Pa. Vickers microhardness ($HV_{0.5}$) tests were conducted at room

**Table 2**
Summary of averaged grain size.

| Code | Annealing temperature (K) | Averaged grain size (μm) |
|---|---|---|
| V-4Cr-4Ti | 1273 | 20 |
| V-3Ta-4Cr-4Ti | 1273 | 20 |
| V-9Ta-4Cr-4Ti | 1373 | 36 |
| V-15Ta-4Cr-4Ti | 1373 | 48 |
| V-22Ta-4Cr-4Ti | 1373 | 51 |

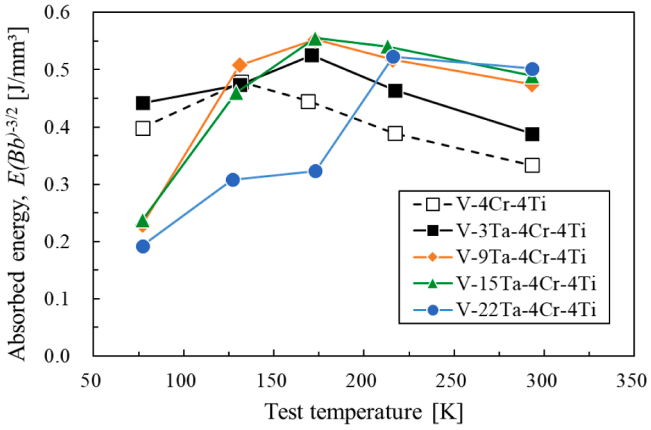


**Fig. 3.** Absorbed energy in the Charpy impact tests. These energies were normalized by specimen width ($B$ = 1.5 mm) and ligament size ($b$ = 1.2 mm), which is $(B \times b)^{3/2} = (1.5 \times 1.2)^{3/2}$.

**Table 3**
Summary of Charpy impact properties.

| Code | USE (J/mm$^3$) | DBTT (K) |
|---|---|---|
| V-4Cr-4Ti | 0.41 | Below 77 |
| V-3Ta-4Cr-4Ti | 0.46 | Below 77 |
| V-9Ta-4Cr-4Ti | 0.51 | 77 |
| V-15Ta-4Cr-4Ti | 0.51 | 77 |
| V-22Ta-4Cr-4Ti | 0.51 | 100 |

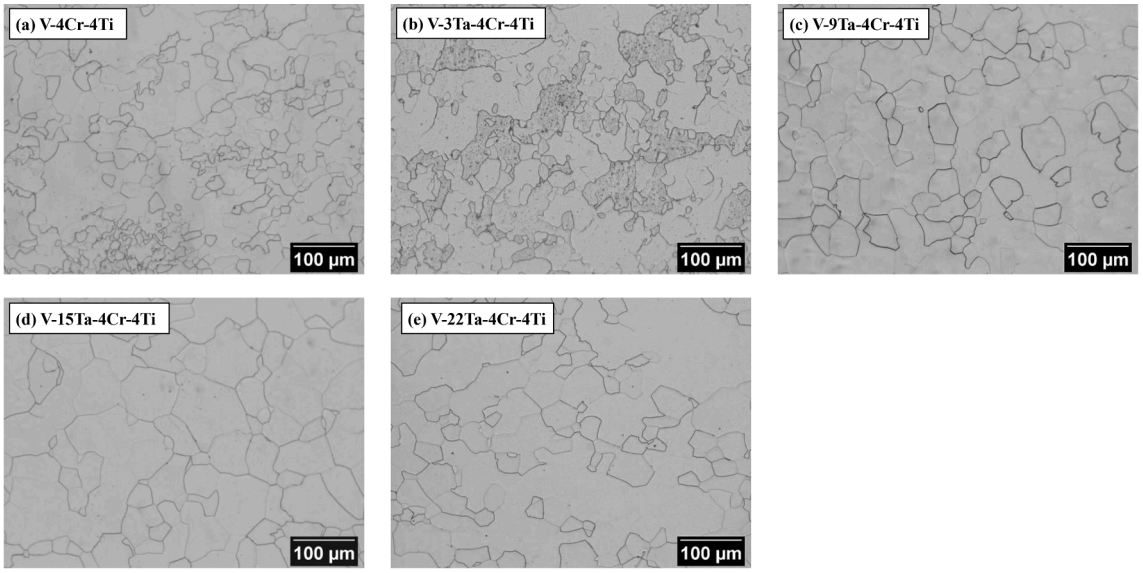


**Fig. 2.** Metallographic images obtained using optical microscopy of the grain structures of (a) V-4Cr-4Ti annealed at 1273 K, (b) V-3Ta-4Cr-4Ti annealed at 1273 K, (c) V-9Ta-4Cr-4Ti annealed at 1373 K, (d) V-15Ta-4Cr-4Ti annealed at 1373 K, and (e) V-22Ta-4Cr-4Ti annealed at 1373 K.

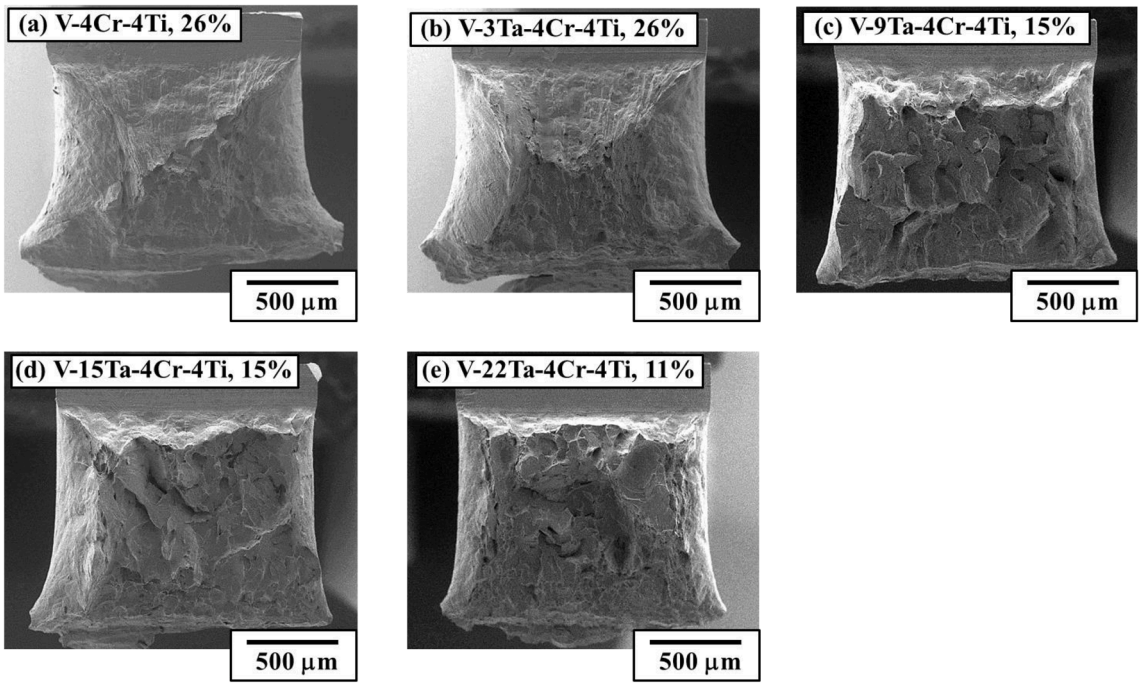


**Fig. 4.** SEM images of the fracture surfaces where data for lateral expansion (LE) are indicated: (a) V-4Cr-4Ti, (b) V-3Ta-4Cr-4Ti, (c) V-9Ta-4Cr-4Ti, (d) V-15Ta-4Cr-4Ti, and (e) V-22Ta-4Cr-4Ti tested at 77 K.

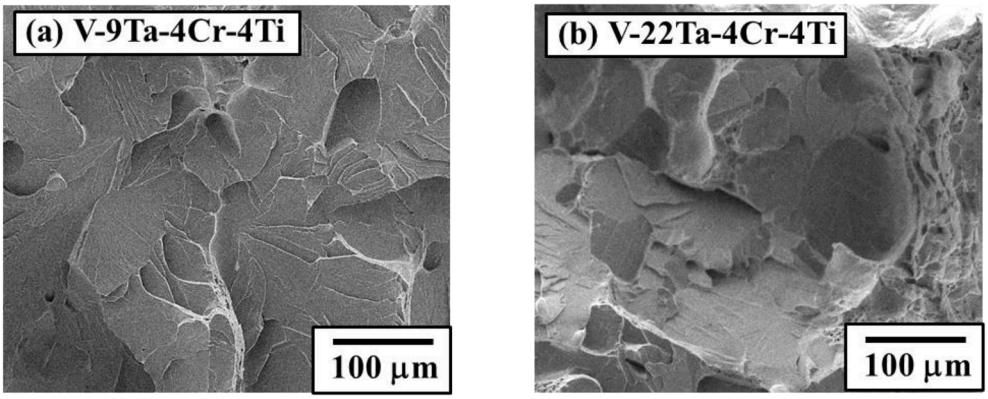


**Fig. 5.** High magnification SEM images of the fracture surfaces tested at 77 K: (a) V-9Ta-4Cr-4Ti, and (b) V-22Ta-4Cr-4Ti.

temperature (in the range 293–298 K), with an indentation load of 4.9 N (500 gf), and a dwell time of 30 s. Hardness was calculated by averaging the results obtained from ten indentation tests. The grain sizes were measured according to the ASTM E112-85 standard [20]. The Charpy V-notch (CVN) specimens had dimensions of $1.5 \times 1.5 \times 20$ mm$^3$, a notch angle of 30°, and a notch depth of 0.3 mm, so that the ligament size $b$ was 1.2 mm. The CVN specimens were adopted for comparison with previous study [10]. Because the rolled V-4Cr-4Ti alloys have the anisotropy on Charpy impact properties [27], the CVN specimens were oriented in the longitudinal–transverse (L-T) direction, so that the crack propagated perpendicular to the rolling direction and along the T direction. CVN specimens were annealed at 1273 K × 1 h for the alloys V-4Cr-4Ti and V-3Ta-4Cr-4Ti, and at 1373 K × 1 h for the three V-$x$Ta-4Cr-4Ti ($x$ = 9, 15, and 22 wt.%) alloys. Charpy impact tests were conducted from 77 K to 293 K using an instrumented falling weight type impact tester at the Institute for Materials Research (IMR), Tohoku University [21]. Initial energy of the tester was 200 J. One sample was tested for each test condition. The test temperatures were measured using a thermocouple at the jig to fix a specimen just before the tests. A specimen and the anvil were cooled together in the cryostat. In order to minimize temperature loss, the specimen was removed from the cryostat together with the anvil and subjected to an impact test. The crosshead speeds of the Charpy impact tests were 5 m/s [22]. The fracture surfaces were observed using scanning electron microscopy (SEM) to evaluate the lateral expansion (LE) and determine the fracture mode. Microstructural observations were conducted using transmission electron microscopy (TEM) and energy dispersive X-ray spectroscopy (EDS) at IMR, Tohoku University. Disk specimens with a diameter of 3 mm were electropolished with 20 % sulfuric acid solution by using a twin-jet polishing machine to make thin films for the TEM observations.

## 3. Results

### 3.1. Hardness and recrystallization

Fig. 1 shows the hardness recovery as a function of the annealing temperature after cold rolling. The minimum hardness was at 1273 K. The minimum values increased with increasing Ta content. Fig. 2 shows the metallographic images obtained using optical microscopy of the grain structures of V-3Ta-4Cr-4Ti annealed at 1273 K, and V-9Ta-4Cr-

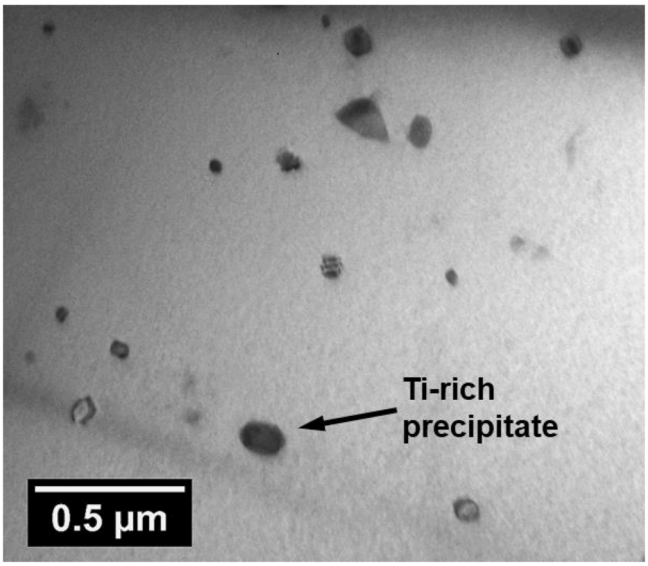


**Fig. 6.** TEM images of V-3Ta-4Cr-4Ti alloys annealed at 1273 K.

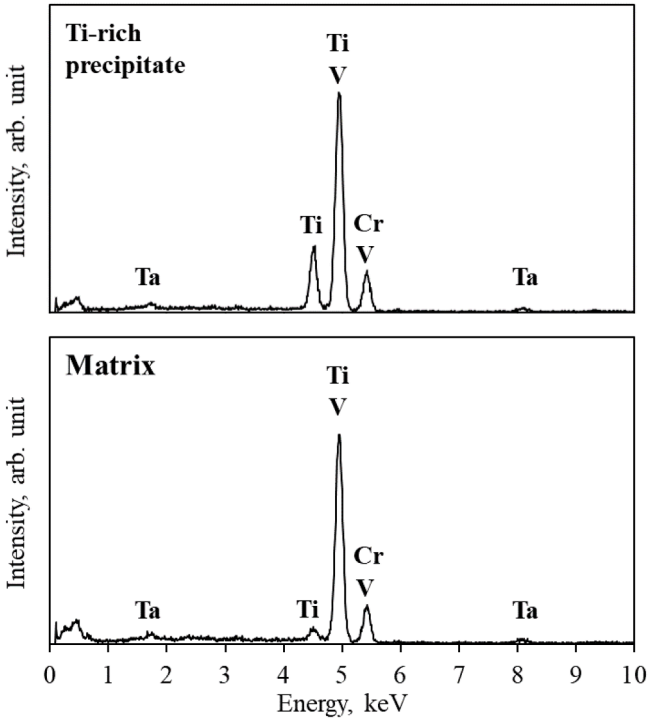


**Fig. 7.** TEM-EDS analysis of the precipitate and matrix.

4Ti and V-22Ta-4Cr-4Ti both annealed at 1373 K. The fully recrystallization temperatures of the alloys were determined based on their hardness and grain structure recovery. The recrystallization temperatures of V-4Cr-4Ti and V-3Ta-4Cr-4Ti were determined to be 1273 K, whereas those of V-9Ta-4Cr-4Ti, V-15Ta-4Cr-4Ti, and V-22Ta-4Cr-4Ti were 1373 K. Thus, the recrystallization temperature increased with increasing Ta content. All Charpy specimens were annealed at their respective recrystallization temperatures. Table 2 summarizes averaged grain size for the alloys annealed at their respective recrystallization temperatures.

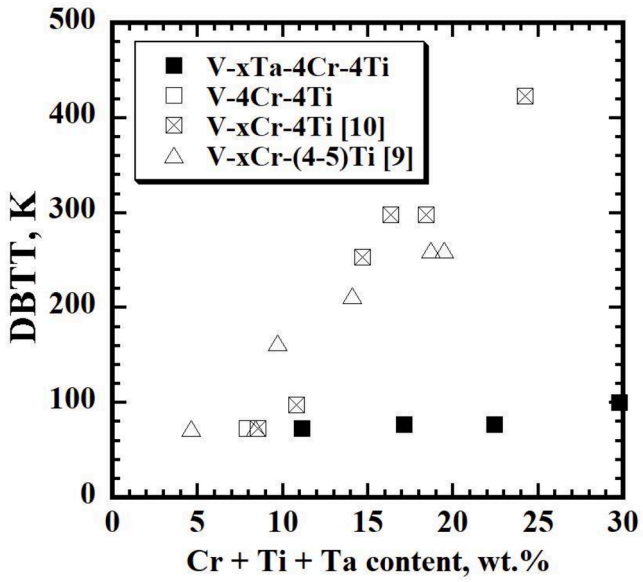


**Fig. 8.** Dependence of DBTT on (Cr + Ti + Ta) content via a comparison of V-*x*Ta-4Cr-4Ti quaternary alloys with high-Cr V-*x*Cr-4Ti and V-*x*Cr-(4–5)Ti ternary alloys [9,10].

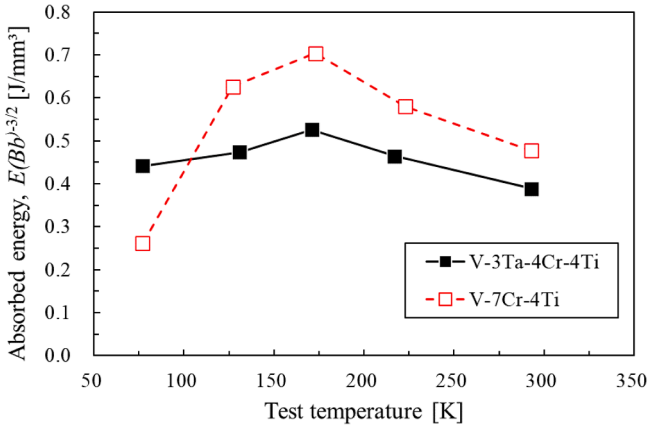


**Fig. 9.** Absorbed energy in the Charpy impact tests comparing V-3Ta-4Cr-4Ti quaternary alloy annealed 1273 K with V-7Cr-4Ti ternary alloy annealed at 1223 K [28].

### 3.2. *Impact properties*

Fig. 3 shows the absorbed energies from 77 K to 293 K. The typical sigmoidal DBT behavior seen V-Cr-Ti system did not be seen because the present investigation only provides as rough estimate of the influence of Ta addition to impact properties. The repeat tests will be required for a more statistical estimate of the transition [23]. In the present study, the DBTT is defined as the temperature where the energy is half of the upper-shelf energy (USE). Table 3 summarizes USEs and DBTTs for the alloys tested in the present study. The USE of V-4Cr-4Ti was 0.41 J/mm$^3$, which was equivalent to that of the reference alloy V-4Cr-4Ti (NIFS-HEAT-2) [24,25]. DBTTs for V-4Cr-4Ti and V-3Ta-4Cr-4Ti alloys were below 77 K; however, DBTTs for V-9Ta-4Cr-4Ti, V-15Ta-4Cr-4Ti and V-22Ta-4Cr-4Ti were above 77 K. Both the USE and the DBTT increased with increasing Ta content. Fig. 4 and Fig. 5 show SEM images of the fracture surfaces of alloys tested at 77 K. Ductile fracture surfaces with dimple patterns and lateral LE > 20 % were observed for V-4Cr-4Ti and V-3Ta-4Cr-4Ti. The fracture surfaces for V-9Ta-4Cr-4Ti, V-15Ta-4Cr-4Ti and V-22Ta-4Cr-4Ti showed a mixture of ductile and brittle

fracture with river patterns.

### 3.3. Microstructural observations

Fig. 6 presents the bright field TEM images of V-3Ta-4Cr-4Ti annealed at 1273 K. V-3Ta-4Cr-4Ti was found to contain precipitates with sizes of 0.05–0.2 μm. Fig. 7 shows the spectrum of TEM-EDS obtained from the matrix and the precipitate. The precipitate was Ti-rich precipitates [26,27]. The spectra of TEM-EDS indicate that there is no significant enrichment of Ta in the matrix as compared with that in the precipitate. Although the current investigation did not reveal (Ti,Ta)CON precipitates, they have been reported in other V-Ti-Cr systems and cannot be ruled out. More detailed research is needed to clarify the characterization of precipitates and distribution of Ta in the matrix of V-3Ta-4Cr-4Ti.

## 4. Discussion

Fig. 8 summarizes the dependence of the DBTT on (Cr + Ti + Ta) content by comparing V-*x*Ta-4Cr-4Ti quaternary alloys with high-Cr V-*x*Cr-4Ti and V-*x*Cr-(4–5)Ti ternary alloys [9,10]. Increasing Cr content increases the DBTT of V-*x*Cr-(4–5)Ti ternary alloys significantly. Although increasing Ta content also increases the DBTT of V-*x*Ta-4Cr-4Ti quaternary alloys, the increment rate of DBTT with increasing Ta content is much lower than that increasing Cr content. The Vickers hardness of V-3Ta-4Cr-4Ti quaternary alloy annealed at 1273 K was 144 HV, which is approximately the same as that of V-7Cr-4Ti ternary alloy annealed at 1273 K [28]. Fig. 9 shows the absorbed energy in the Charpy impact tests for V-3Ta-4Cr-4Ti and V-7Cr-4Ti. The USE of V-7Cr-4Ti was 0.60 J/mm$^3$, which was higher than that of V-3Ta-4Cr-4Ti. However, the DBTT for V-7Cr-4Ti was above 77 K. For the V-Ta-4Cr-4Ti quaternary alloys, both the USE and the DBTT increased with increasing Ta content. To maintain the same DBTT as V-4Cr-4Ti ternary alloy, the addition of 3 wt.% (approximately 1 at.%) Ta is an appropriate amount for use in blanket structural materials for advanced fusion reactors. In a previous study on effect of substitutional solid solution elements (W, Mo, Al, Mn and Cu) on the high temperature strength of 17Cr-14Ni austenitic steels [29], the lattice distortion induced by solute elements improved the steady creep rate. Additions of Mo and W were effective in improving creep strength in austenitic heat resisting steels. Thus, the addition of 3 wt.% Ta is also expected to improve the creep rupture strength of V-4Cr-4Ti ternary alloy.

This study revealed that the addition of 3 wt.% Ta resulted in solid solution strengthening without the degradation of Charpy impact properties, such as embrittlement, which is one of the key factors that determines the lower operating temperature limit [7]. In general, having favorable Charpy impact properties means having a long life until irradiation embrittlement. It has been reported that the swelling of V-base binary alloys depends on the atomic size factor of the solute atoms [30]. Mo and niobium (Nb) in the V matrix are oversized solutes, which suppress swelling. As Ta is also an oversized solute, it is expected to suppress swelling as well. The addition of 3 wt.% Ta has the advantage of expanding both the upper and the lower operating temperature limits of V-4Cr-4Ti ternary alloy.

Having a solid solubility limit of 9 at.% in the V-Ta phase diagram [19], Ta can form the Laves phase ($V_2Ta$) in the V matrix. The phase stabilities of 8–12Cr ferritic steels such as 12Cr-1Mo-V-W (HT9), 9Cr-1Mo-V-Nb (T-91), and 8Cr-2W-V-Ta (F82H) have previously been reported, as well as Laves phase ($Fe_2Mo$, $Fe_2W$) formation during thermal aging [31]. The Laves phase precipitates formed at grain boundaries during thermal aging caused the degradation of Charpy impact properties, leading to embrittlement [32,33]. While there was no significant enrichment of Ta in the matrix as compared with that in the precipitate for the V-3Ta-4Cr-4Ti quaternary alloy (Figs. 5 and 6), thermal aging may still result in the formation of the Laves phase. In order to determine the optimum Ta content, conducting creep tests on the V-3Ta-4Cr-4Ti quaternary alloy is necessary. Further investigation on effects of thermal aging is also warranted.

## 5. Conclusions

The effect of Ta addition on the Charpy impact properties of V-*x*Ta-4Cr-4Ti alloys ($x$ = 3, 9, 15, and 22 wt.%) was investigated. Both the USE and DBTT increased with increasing Ta content. The addition of 3 wt.% Ta resulted in solid solution strengthening without the degradation of Charpy impact properties. The addition of 3 wt.% Ta (V-3Ta-4Cr-4Ti) is therefore an appropriate amount for use in blanket structural materials used in nuclear fusion reactors. From the TEM-EDS analysis, it was observed that there is no significant enrichment of Ta in the matrix as compared with that in the precipitate. However, thermal aging may result in the formation of the Laves phase, causing a degradation of Charpy impact properties. Thus, the characterization of precipitates, thermal aging studies, and creep tests on the V-3Ta-4Cr-4Ti quaternary alloy will be required in the future to determine the optimum Ta content.

### *CRediT authorship contribution statement*

**Takeshi Miyazawa:** Conceptualization, Investigation, Writing – original draft. **Haruka Saito:** Data curation. **Yoshimitsu Hishinuma:** Investigation. **Takuya Nagasaka:** Investigation. **Takeo Muroga:** Project administration. **Jingjie Shen:** Investigation. **Yasuki Okuno:** Data curation. **Hao Yu:** Data curation. **Ryuta Kasada:** Data curation. **Akira Hasegawa:** Project administration.

### Declaration of Competing Interest

The authors declare that they have no known competing financial interests or personal relationships that could have appeared to influence the work reported in this paper.

### *Acknowledgment*

The authors thank Mr. Shun Ito who is a technical staff member at the IMR, Tohoku University, for support with the TEM/EDS observations. This work was conducted using the budgets of the NIFS Collaboration Research Program (NIFS20KEMF172) and JSPS KAKENHI, Grant Number 21 K03505.

We would like to thank Editage (www.editage.com) for English language editing.

### References

[1] T. Muroga, Comprehensive Nuclear Materials 4 (2012) 391–406.
[2] D.L. Smith, B.A. Loomis, D.R. Diercks, J. Nucl. Mater. 135 (1985) 125–139.
[3] D.L. Smith, H.M. Chung, B.A. Loomis, H. Matsui, S.N. Votinov, W. Van Witzenburg, Fusion Eng. Des. 29 (1995) 399–410.
[4] H. Matsui, K. Fukumoto, D.L. Smith, H.M. Chung, W. Van Witzenburg, S. N. Votinov, J. Nucl. Mater. 233–237 (1996) 92–99.
[5] B.A. Loomis, D.L. Smith, J. Nucl. Mater. 179–181 (1991) 783–786.
[6] D.L. Smith, H.M. Chung, B.A. Loomis, H.-C. Tsai, J. Nucl. Mater. 233–237 (1996) 356–363.
[7] S.J. Zinkle, N.M. Ghoniem, Fusion Eng. Des. 51–52 (2000) 55–71.
[8] H.M. Chung, B.A. Loomis, D.L. Smith, J. Nucl. Mater. 212–215 (1994) 772–777.
[9] B.A. Loomis, H.M. Chung, L.J. Nowicki, D.L. Smith, J. Nucl. Mater. 212–215 (1994) 799–803.
[10] K. Sakai, M. Satou, M. Fujiwara, K. Takahashi, A. Hasegawa, K. Abe, J. Nucl. Mater. 329–333 (2004) 457–461.
[11] T. Miyazawa, Y. Hishinuma, T, Nagasaka and T. Muroga: Fusion Eng. Des. **165** (2021) 112191.
[12] S. Cierjacks, K. Ehrlich, E.T. Cheng, H. Conrads, H. Ullmaier, Nucl. Sci. Eng. 106 (1990) 99–113.
[13] N. Iwao, T. Kainuma, T. Suzuki, R. Watanabe, J. Less-Common Met. 83 (1982) 205–217.
[14] N. Iwao, T. Kainuma, R. Watanabe, T. Shimomura, Trans. Jan. Inst. Met. 20 (1979) 172–180.
[15] B.R. Rajala, R.J. VanThyne, J. Less-Common Met. 3 (1961) 489–500.
[16] N. Iwao, T. Kainuma, T. Suzuki, R. Watanabe, J. Less-Common Met. 83 (1982) 219–225.

[17] T. Nagasaka, T. Muroga, M. Imamura, S. Tomiyama, M. Sakata, Fusion Technol. 39 (2001) 659–663.
[18] T. Nagasaka, T. Muroga, Y. Wu, M. Imamura, J. Plasma Fusion Res. SERIES 5 (2002) 545–550.
[19] Phase diagrams of binary vanadium alloys, edited by J.F. Smith, ASM International.
[20] Astm, E112–85, Standard methods for determining the average grain size: Annual Book of ASTM Standards Sect, Met. Test Methods and Anal. Proc. (1986) 227–290.
[21] H. Kayano, H. Kurishita, M. Narui, M. Yamazaki, Ann. Chem. Fr. 16 (1991) 309.
[22] H. Kurishita, T. Yamamoto, M. Narui, H. Suwarno, T. Yoshitake, Y. Yano, M. Yamazaki, H. Matsui, J. Nucl. Mater. 329–333 (2004) 1107–1112.
[23] R. Chaouadi, J. Nucl. Mater. 360 (2007) 75–91.
[24] T. Nagasaka, T. Muroga, H. Watanabe, T. Miyazawa, M. Yamazaki, K. Shinozaki, J. Nucl. Mater. 442 (2013) S364–S369.
[25] T. Miyazawa, T. Nagasaka, Y. Hishinuma, T. Muroga, Y. Li, Fusion Sci. Technol. 60 (2011) 407–411.
[26] N.J. Heo, T. Nagasaka, T. Muroga, J. Nucl. Mater. 325 (2004) 53–60.
[27] T. Nagasaka, N.J. Heo, T. Muroga, M. Imamura, Fusion Eng. Des. 61–62 (2002) 757–762.
[28] K. Sakai: Master thesis (2004), Tohoku University.
[29] T. Matsuo, T. Shinoda, R. Tanaka, Tetsu-to-Hagané 63 (1977) 980–989.
[30] H. Matsui, H. Nakajima, S. Yoshida, J. Nucl. Mater. 205 (1993) 452–459.
[31] M. Tamura, H. Hayakawa, A. Yoshitake, A. Hishinuma, T. Kondo, J. Nucl. Mater. 155–157 (1988) 620–625.
[32] M. Tamura, K. Shinozuka, H. Esaka, S. Sugimoto, K. Ishizawa, K. Masamura, J. Nucl. Mater. 283–287 (2000) 667–671.
[33] K. Shiba, H. Tanigawa, T. Hirose, H. Sakasegawa, S. Jitsukawa, Fusion Eng. Des. 86 (2011) 2895–2899.